

# The Tidal Tails of the Ultra-Faint Globular Cluster Palomar 1

M.Niederste-Ostholt<sup>1\*</sup>, V. Belokurov<sup>1</sup>, N.W. Evans<sup>1</sup>, S. Koposov<sup>1,2</sup>, M. Gieles<sup>1</sup>, M.J. Irwin<sup>1</sup>

<sup>1</sup> *Institute of Astronomy, Madingley Rd, Cambridge, CB3 0HA*

<sup>2</sup> *Sternberg Astronomical Institute, Universitetskii pr. 13, 119992 Moscow, Russia*

May 2010

## ABSTRACT

Using the Optimal Filter Technique applied to Sloan Digital Sky Survey photometry, we have found extended tails stretching about  $1^\circ$  (or several tens of half-light radii) from either side of the ultra-faint globular cluster Palomar 1. The tails contain roughly as many stars as does the cluster itself. Using deeper Hubble Space Telescope data, we see that the isophotes twist in a characteristic S-shape on moving outwards from the cluster centre to the tails. We argue that the main mechanism forming the tails may be relaxation driven evaporation and that Pal 1 may have been accreted from a now disrupted dwarf galaxy  $\sim 500$  Myr ago.

**Key words:** globular clusters: tidal disruption – globular clusters: individual (Palomar 1)

## 1 INTRODUCTION

Fig. 1 shows a Sloan Digital Sky Survey (SDSS) image of the sparsely populated, young halo globular cluster Palomar 1. It was originally discovered by Abell (1955), and lies 3.7 kpc above the Galactic disk and 17.3 kpc from the Galactic Centre (Rosenberg et al. 1998a,b; Sarajedini et al. 2007). Its size and low luminosity are very similar to recently discovered Milky Way globular clusters, such as Segue 3, Koposov 1 and 2 (Belokurov et al. 2010; Koposov et al. 2007), as well as Whiting 1, AM 4 and E 3 (Whiting et al. 2002; Carraro 2005; van den Bergh et al. 1980; Carraro 2009). The Sloan Digital Sky Survey color-magnitude diagram (CMD) of Pal 1 shows a red clump, a main sequence turn-off and a well defined main-sequence down approximately two magnitudes from the turn-off. The giant branch on the other hand is very sparsely populated (Borissova & Spassova 1995; Sarajedini et al. 2007).

Owing to its unusually flat mass function, Rosenberg et al. (1998a) suggested that Pal 1 has either experienced strong dynamical evolution (either tidal shocks or evaporation) or that its initial mass function is significantly different from other halo clusters. van den Bergh (2000) notes that Pal 1 is part of a group of young halo globular clusters (including Palomar 12, Ruprecht 106, IC 4499, Arp 2, Terzan 7, Palomar 3, Palomar 4, Eridanus, Fornax 4, NGC 4590). It has often been suggested that these young globular clus-

ters were formed in dwarf companions of the Milky Way, which have since been accreted and destroyed, leaving their clusters behind. For example, Crane et al. (2003) proposed that Pal 1 is part of the Monoceros ring (along with NGC 2808, NGC 5286, NGC 2298), whilst Belokurov et al. (2007) suggested it may be associated with the accretion event that formed the Orphan Stream (along with Ruprecht 106 and possibly Terzan 7).

Pal 1, together with Segue 3, Koposov 1 and 2, Whiting 1, E 3, and AM 4, comprise *an ultra-faint population* of globular clusters. Pal 1 is the nearest of the six contained within the SDSS footprint (though E3 is still closer to the Sun and Galactic Centre). Compared to the other young globular clusters, Pal 1 is the faintest and smallest. Its tiny size and low luminosity (and hence presumably low mass) make it an attractive target to look for the effect of tides or dynamical evolution, which is the purpose of this *Letter*.

## 2 TAIL DETECTION

Pal 1 is located at  $(l, b) = (130.1^\circ, 19.0^\circ)$ . It has an absolute magnitude of  $M_V = -2.5 \pm 0.5$  and a half-light radius of  $R_h \approx 2.2$  pc and its heliocentric radial velocity is  $-82.3 \pm 3.3$   $\text{kms}^{-1}$  (Rosenberg et al. 1998a,b; Ortolani & Rosino 1985). Pal 1 lies within an SDSS data release 7 stripe (Abazajian et al. 2009), covering  $2.5^\circ$  in galactic longitude and  $11.3^\circ$  in galactic latitude. Henceforth, all SDSS magnitudes are corrected for extinction using the maps of Schlegel et al. (1998).

The panels of Fig. 2 show  $82 \times 18$  pixel maps of the

\* E-mail:mno@ast.cam.ac.uk

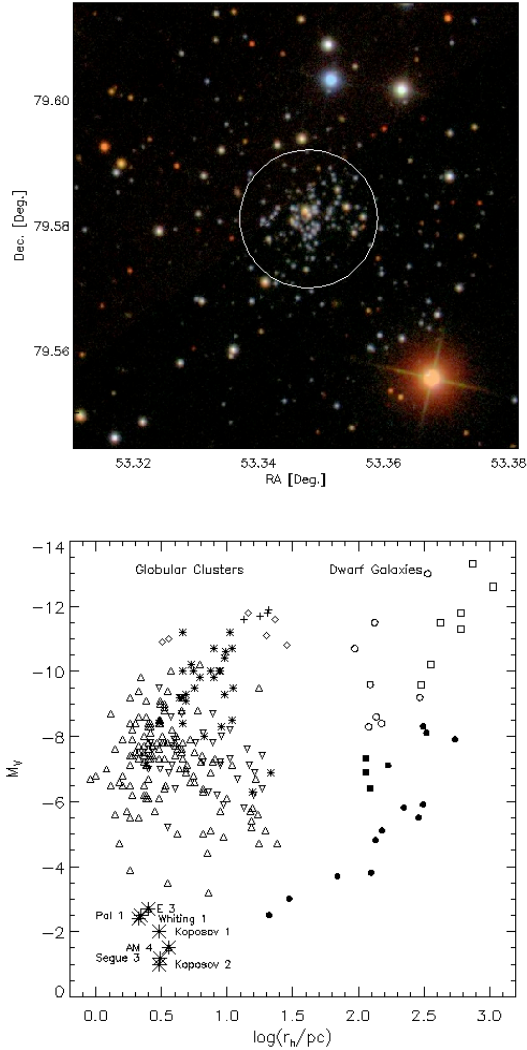


**Figure 1.** Upper: SDSS image of Pal 1. The white circle marks the half-light radius of the cluster found by Rosenberg et al. (1998a). Lower: Absolute magnitude versus half-light radius for various globular clusters and dwarf galaxies. Pal 1 is among a group of ultra-faint globular clusters in the lower left corner.

the density of stars around Pal 1, an estimate of the possible smooth underlying distribution of stars, the distribution of galaxies in the area, as well as the mean  $g$ -band extinction. Pal 1 is clearly visible as an overdensity in the topmost panel. To search for stars torn from Pal 1, we employ the optimal filter technique which works by calculating conditional probabilities of cluster and foreground membership from densities in colour-magnitude space, known as Hess diagrams. From this weighted distribution, a smooth distribution of field stars is then subtracted (see e.g. Odenkirchen et al. 2003; Niederste-Ostholt et al. 2009). The field star density is estimated by removing a  $0.3^\circ \times 0.3^\circ$  box around the cluster, replacing it by a patch at  $(\ell, b) = (131.1^\circ, 22.0^\circ)$ , and smoothing the resultant distribution with a Gaussian kernel of FWHM 15 pixels and a box-car smoothing over 2 pixels.

The left-hand panel of Fig. 3 shows the Hess difference between stars within  $0.16^\circ$  and those further than  $0.5^\circ$  from the centre of Pal 1. The mask shown encloses both the main

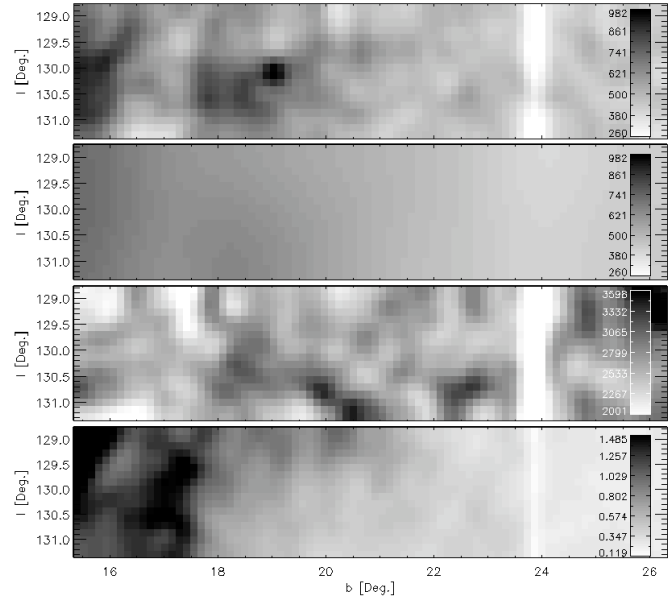


**Figure 2.** Upper: The density of stars around Pal 1 lying within a CMD mask drawn around the cluster’s distribution (see Fig. 3 left panel). The conversion of grey-scale to stars per degree is given in the bar on the right. Upper middle: An estimate of the smooth field star population around Pal 1 using the same grey-scale. Lower middle: The density of galaxies around Pal 1. Lower: The mean  $g$ -band extinction per pixel around Pal 1.

sequence and the red clump, though the inclusion of the red clump makes little difference to our results as the giant-branch is so poorly populated. The mask closely follows the main sequence at the red edge but allows more leeway on the blue side. This is done since the contamination from disk and halo stars is more severe at the red side of the distribution. The ratio of the Hess diagrams is used as the weights in the optimal filter analysis.

Fig. 4 shows the results of the optimal filter analysis. The distribution is smoothed with a Gaussian kernel over 3 pixels. Pal 1 stands out as the most significant overdensity in the field but there are significant overdensities extending from it towards higher and lower galactic latitudes. There is also a high signal region at the lower edge of the plot, but follow-up analysis shows this to be unrelated to the cluster and likely to be an artefact caused by the high extinction in this region, together with edge effects. The lower panel of Fig. 4 shows the results with a higher spatial resolution ( $123 \times 27$  pixels), smoothed over 3 pixels. Again, the tails are noticeable in an otherwise nearly noise-free area. Color-magnitude analyses of the tails are shown in Fig. 3. There are suggestive similarities between the main body of Pal 1 and this debris. The stars in both extensions are concentrated around Pal 1’s main sequence turn-off with a faint continuation down the main sequence.

Pal 1 does not appear to be embedded in a noisy field. It is not possible to conclude from the optimal filter analysis whether or not it was once part of a dwarf companion. Of course, such a stream may be hidden by the small field-of-view available, or it may already have dispersed.

There exist deep *Hubble Space Telescope* (HST) ACS data covering Pal 1 (Sarajedini et al. 2007), which allow us

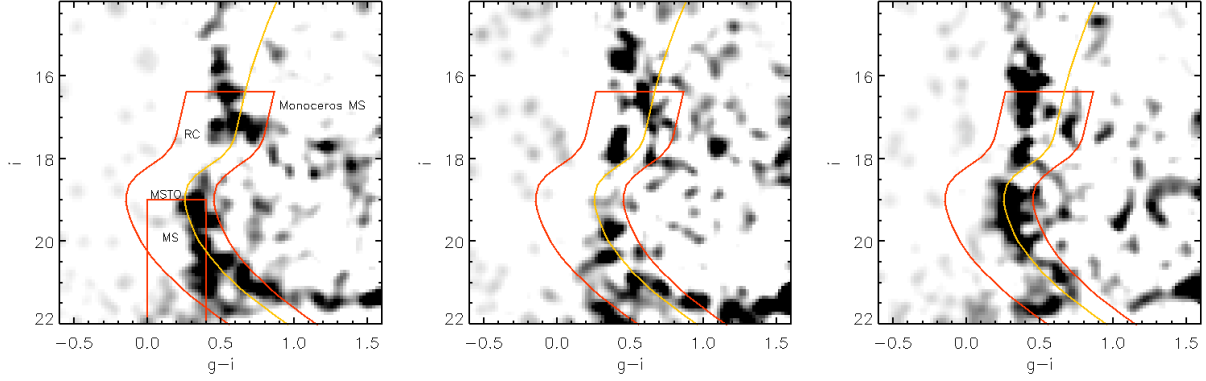


**Figure 3.** Left: Hess difference between stars within  $0.16^\circ$  from the centre of Pal 1 and stars further than  $0.5^\circ$  from the centre (field stars). The mask is used to select stars for the optimal filter analysis, with stars outside the mask having zero weight. Also shown is the rectangular box mask used in the star-count analysis. The ridgeline overplotted for comparison purposes is that of the metal-poor globular cluster M92 (Clem 2005), offset to Pal 1’s distance modulus. Pal 1’s main sequence (MS), main sequence turn-off (MSTO), and red clump (RC) are labelled. The structure visible approximately 3 magnitudes brighter than Pal 1 is probably the main sequence of the Monoceros ring. Center: The Hess difference diagram of stars in the northern (higher latitude) tail of debris around Pal 1 together with the CMD mask used to select cluster stars. Right: The same, but for the southern (lower latitude) tail. In both cases, the Hess diagram of field stars in the area (defined as stars with  $b > 21.5^\circ$  and  $b < 17.5^\circ$ ) is subtracted. Both stream candidates show an overdensity of stars near Pal 1’s main-sequence turn-off with a slight extension down the main sequence. In all cases, the ridgeline of the metal-poor globular cluster M92 (Clem 2005) is overplotted in yellow.

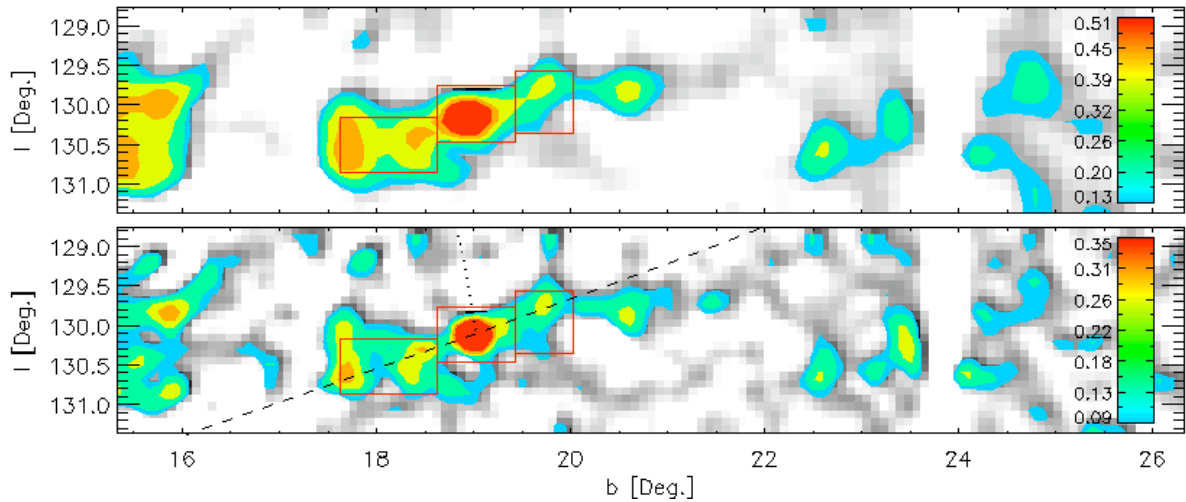


**Figure 4.** Upper: Optimal filter technique applied to SDSS data centred on Pal 1. The area is divided into  $82 \times 18$  pixels and smoothed with a Gaussian kernel of  $FWHM = 3$  pixels. The coloured contours show 1.5, 2, 3, 4, 5 $\sigma$  levels above the mean. The density is normalized to the average pixel density within  $0.08^\circ$  of the centre of Pal 1. The colour within the contours can be converted into normalized pixel density by the key. The cluster clearly stands out in the centre of the plot. There are two overdensities connected to Pal 1, extending away from it. Aside from a prominent overdensity at lower latitudes, the field is quite smooth. The boxes mark the areas contain probable debris of Pal 1 and whose Hess difference diagrams are shown in Fig. 3. Bottom: Optimal filter analysis with a higher spatial resolution ( $123 \times 27$  pixels). The structural integrity of the two extensions from Pal 1 is preserved and they appear to be streams showing a characteristic S-shape near the cluster. The dashed line is a great circle fitted to the possible debris structure with a pole at  $(\ell, b) = (-132.2^\circ, 21.3^\circ)$ . The dotted line shows the direction towards the Galactic centre.

to explore the central regions more closely. By applying our source extraction to the HST images, we select cluster stars based on their position in color-magnitude space, as shown in the inset in Fig. 5. We then overplot the density contours derived from the HST data on a higher resolution ( $574$  by  $126$  pixels, smoothed over 1 pixel) version of the optimal filter analysis. This high resolution plot of the central  $0.2^\circ \times 0.2^\circ$  does not allow us to identify any debris. However, we can see that the central region of the cluster is elongated, pointing towards the Galactic Centre, and that the cluster

stars are spread over several half-light radii ( $R_h \approx 0.01^\circ$ ). The outer isodensity contours, given by the optimal filter technique, twist and align with the direction of the debris. Such an S-shaped misalignment between tidal debris and the elongation of the central regions is observed in simulations when the object is near the apocentre of its orbit (see for example the bottom row of Fig. 4 in Johnston et al. 2002).

To estimate the number of stars in the tails, we use a coordinate system  $(\ell', b')$ , in which the extensions lie along a great circle (see lower panel of Fig. 4). In this system, Pal

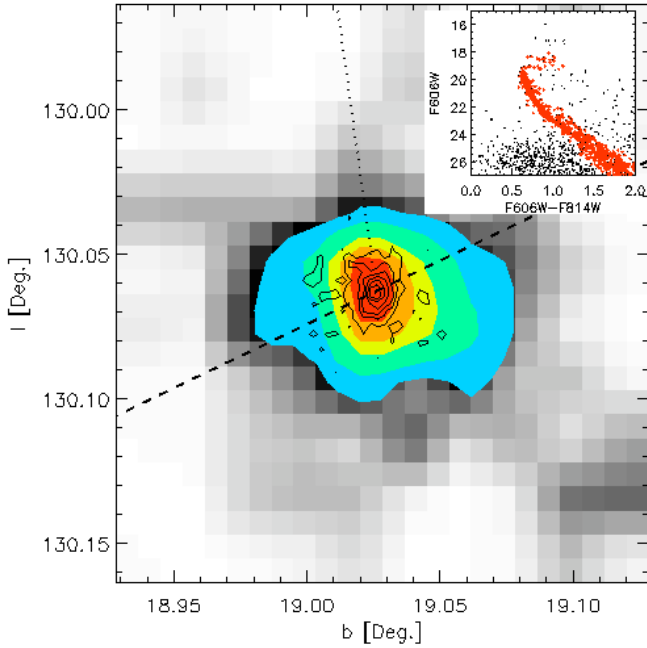


**Figure 5.** Inset: CMD of the HST observations of Pal 1 in the F606W and F814W filters (approximately  $V$  and  $I$ ). The red dots mark the stars which are included in the black-line contours. Main: High resolution optimal filter analysis (grey-scale and colored contours) with HST contours overplotted. The coloured contours show the 0.5, 1.5, 3, 4, 5 $\sigma$  levels above mean density in the field. This corresponds to densities (in number of stars per square arc minute) of 78.1, 156.3, 234.4, 312.5, 390.6, 468.8. The central region of the cluster is elongated and points towards the Galactic Centre (dotted line). The dashed line shows the direction of the debris.

$l$ 's possible debris lie at roughly constant latitude ( $b' \approx 0^\circ$ ). The top panel of Fig. 6 shows the density of stars in a  $2^\circ$  area around Pal 1 in this new coordinate system. There are 9 bins along, and 21 bins perpendicular to, the stream direction. By using larger bins in the direction along the stream, we can assess the significance of the enhancement around Pal 1. The influence of the cluster itself has been removed from this plot by excluding stars that are within 4 half-light radii ( $\sim 0.04^\circ$ ) of the cluster centre. To amplify the signal of Pal 1 stars, this plot is restricted to stars lying in the rectangular box in color-magnitude space shown in Fig. 3 left panel, which picks up the Pal 1 main sequence turn-off and the blue edge of the main sequence. This avoids contamination from the field stars, which lie slightly to the red of the main sequence. To account for possible contamination in this plot, we subtract a background estimate, derived by applying a linear fit to each column of constant  $l'$ , to arrive at the upper panel of Fig. 6. The stream stands out as a continuous overdensity of pixels along  $b' \approx 0$ . It is now straightforward to count the number of stream stars present by summing the weighted, background subtracted counts in bins of constant latitude  $b'$  as shown in the lower panel of Fig. 6. There is a significant spike at  $b' \approx 0^\circ$ , which we identify as the tails of Pal 1. There seem to be on order the same number of stars in the tails (approximately 70) as in the cluster (approximately 85), suggesting that the mass in the tails is comparable to the mass in the cluster.

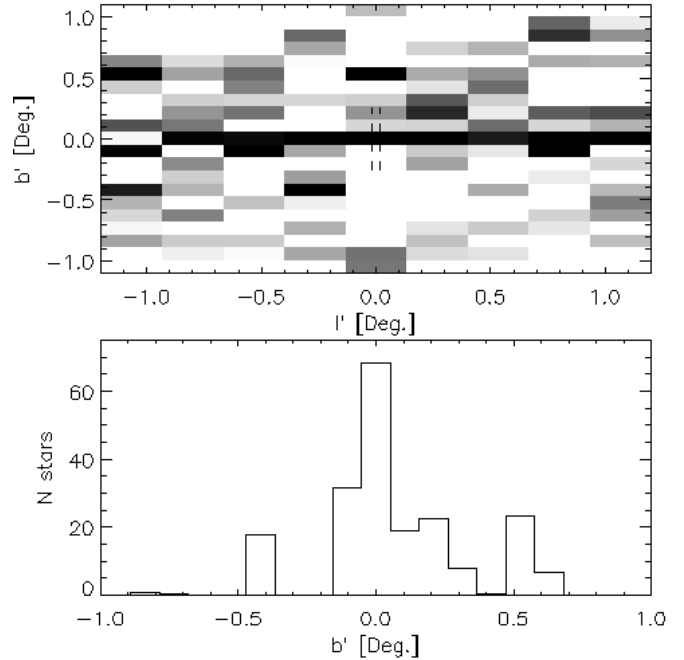


**Figure 6.** Top: Background subtracted density of stars in the  $(l', b')$  coordinate system, which is defined by its pole at  $(l, b) = (-132.2^\circ, 21.3^\circ)$  and origin at Pal 1's location. The core of the cluster is shown as two vertical lines. We identify the continuous high density region lying along  $b' \approx 0^\circ$  as the Pal 1 streams. Bottom: Number of stars vs. latitude. There is a significant spike at  $b' \approx 0^\circ$  suggesting there are approximately 60 stars in the debris, comparable to the number of stars within Pal 1.

### 3 CONCLUSIONS

We have discovered probable tails around the globular cluster Pal 1 in Sloan Digital Sky Survey data. The tails cover at least  $2^\circ$  on the sky and extend northward and southward from the cluster centre, possibly up to  $\approx 80$  half-light radii. The tails contain roughly as many stars as does the cluster itself. *Hubble Space Telescope* data reveal that the central parts of the cluster are clearly elongated, with cluster stars spread over several half-light radii. The tails constrain the direction of Pal 1's projected proper motion, but this, together with its measured radial velocity, is not sufficient to establish meaningful constraints on the orbital parameters of Pal 1.

Pal 1 is a prototype of the population of ultrafaint globular clusters with  $M_v$  fainter than  $-3$ . This also includes Segue 3, Koposov 1 and 2, as well as Whiting 1, E3 and AM 4. If the ultrafaint globular clusters are born in their present state, then they would evaporate within 1 Gyr (Rosenberg et al. 1998a; Koposov et al. 2007). Hence, it would be unlikely that they survived long enough for us to see them, unless a large number of such clusters are born like this continuously. It is much more likely that globular clusters evolve into the ultrafaint régime, either through tides or through evaporation causing catastrophic loss of stars. Mass loss due to evaporation is accelerated when the cluster orbits in a tidal field, as for example is the case if an accreted dwarf galaxy originally hosted the cluster.

Could the tails of Pal 1 be caused primarily by evap-

oration? First, assuming a mass-to-light ratio of  $\sim 2$  gives a present cluster mass of  $\sim 1400 M_{\odot}$ . Pal 1 has a half-mass relaxation time (Spitzer & Hart 1971) of  $t_r \sim 0.16$  Gyr. Based on the results of dynamical models, a lower-limit to the mass-loss rate due to relaxation driven evaporation is  $1.4 M_{\odot} \text{ Myr}^{-1}$  for an assumed circular orbit (Baumgardt & Makino 2003), which scales like  $(1 - e)^{-1}$  for an orbit with eccentricity  $e$ . Assuming that stars escape and drift with velocities  $\sim 1 \text{ kms}^{-1}$  as suggested by eq. (18) of (Küpper et al. 2010), then the mass within a length  $L_{\text{Tail}} \sim 400 \text{ pc}$  of the tidal tails ( $\sim 2^{\circ}$  on the sky) is  $M_{\text{Tail}} \sim \dot{M} \times L_{\text{Tail}}/\sigma \sim 560 M_{\odot}$  for a circular orbit. This rises to  $\sim 1100 M_{\odot}$  for an eccentricity  $e = 0.5$ , which is comparable to the mass of the cluster. Secondly, the Jacobi radius at Galactocentric radius of  $\sim 17 \text{ kpc}$  for an object of the mass of Pal 1 is  $r_J \sim 26 \text{ pc}$ , so that  $r_h/r_J \gtrsim 0.1$ . This is surprisingly low for a dynamically evolved system. Baumgardt et al. (2010) find that the expected  $r_h/r_J \sim 0.3$  for extended and low-mass Galactic globular clusters. This suggests that the cluster is underfilling its Roche-surface. Both arguments favour evaporation rather than disk shocking as the main formation mechanism.

Pal 1 is therefore a rather different object to Pal 5, which is well-known to have extended tails (Odenkirchen et al. 2003). Pal 5 is overfilling its Roche surface and its tails are believed to have formed primarily by disk shocking (Dehnen et al. 2004). Certainly, given its present state of disruption, Pal 1 must have passed within 8 kpc of the Galactic Centre in order for disk shocking to account for the tidal tails, as judged by Figure 14 of Vesperini & Heggie (1997).

If Pal 1 has been evolving in a satellite galaxy with a stronger tidal field, we expect it to have it a high density with respect to its current Galactocentric radius. This may explain why it is currently underfilling its Roche surface. However, the accretion must then have happened very recently, because the relaxation time is so low that adjustment to the new tidal field would happen quickly. For a cluster that is not too severely affected by the tidal field its (half-mass) relaxation time,  $t_r$ , increases linearly with its age (Hénon 1965; Baumgardt et al. 2002) because of expansion driven by binaries and 2-body relaxation. This expansion is ultimately stopped by the tidal field and then  $t_r$  decreases with age (Hénon 1961). We assume that the cluster was in this Roche-lobe filling evolution in the original host galaxy. Let us denote by sub-script 0 the time of accretion, and assume that Pal 1 after accretion in the Milky Way started expanding again due to the weaker tidal field. Gieles et al. (2010) showed that for globular clusters  $t_r = 0.3t$ , where  $t$  is the age of the cluster. This means that

$$t_r \approx t_{r,0} + 0.3(t - t_0) \Rightarrow t - t_0 \approx 3.3(t_r - t_{r,0}) \quad (1)$$

Putting  $t_{r,0} \approx 0$  gives a rough upper limit on the accretion time of  $\sim 500 \text{ Myr}$  in the past.

## ACKNOWLEDGMENTS

MNO is funded by the Gates Cambridge Trust, the Isaac Newton Studentship fund and the Science and Technology Facilities Council (STFC), whilst VB acknowledges financial support from the Royal Society. We thank M.G. Walker for

helpful advice and support and the referee, Laszlo Kiss, for constructive feedback.

Funding for the SDSS and SDSS-II has been provided by the Alfred P. Sloan Foundation, the Participating Institutions, the National Science Foundation, the U.S. Department of Energy, the National Aeronautics and Space Administration, the Japanese Monbukagakusho, the Max Planck Society, and the Higher Education Funding Council for England. The SDSS Web Site is <http://www.sdss.org/>. The paper is partly based on observations made with the NASA/ESA Hubble Space Telescope, obtained from the data archive at the Space Telescope Institute. STScI is operated by the association of Universities for Research in Astronomy, Inc. under the NASA contract NAS 5-26555.

## REFERENCES

- Abazajian, K.N. et al. 2009, *ApJS*, 182, 543  
 Abell, G.O. 1995, *PASP*, 67, 258  
 Baumgardt H., Hut P., Heggie D. C., 2002, *MNRAS*, 336, 1069  
 Baumgardt, H., & Makino, J. 2003, *MNRAS*, 340, 227  
 Baumgardt, H., Parmentier, G., Gieles, M., & Vesperini, E. 2010, *MNRAS*, 401, 1832  
 Belokurov, V., et al. 2007, *ApJ*, 658, 337  
 Belokurov, V., et al. 2010, *ApJL*, 712, 103  
 Borissova, J., & Spassova, N. 1995, *A&AS*, 110, 1  
 Carraro, G. 2005, *ApJ*, 621, 61L  
 Carraro, G. 2009, *AJ*, 137, 3809  
 Clem, J.L., 2005, PhD Thesis, Univ. Victoria  
 Crane, J.D., Majewski, S.R., Rocha-Pinto, H.J., Frinchaboy, P.M., Skrutskie, M.F., Law, D.R. 2003, *ApJ*, 594, L119  
 Dehnen, W., Odenkirchen, M., Grebel, E. K., & Rix, H.-W. 2004, *AJ*, 127, 2753  
 Gieles, M., Baumgardt, H., Heggie, D., & Lamers, H. 2010, *MNRAS*, in press (arXiv:1007.2333)  
 Hénon M., 1961, *Annales d'Astrophysique*, 24, 369  
 Hénon M., 1965, *Annales d'Astrophysique*, 28, 62  
 Inman, R. T., & Carney, B. W. 1987, *AJ*, 93, 1166  
 Johnston, K. V., Choi, P. I., Guhathakurta, P. 2002, *AJ*, 124, 127  
 Kinman, T.D., & Rosino, L. 1962, *PASP*, 74, 499  
 Koposov, S., et al. 2007, *ApJ*, 669, 337  
 Küpper, A. H. W., Kroupa, P., Baumgardt, H., & Heggie, D. C. 2010, *MNRAS*, 401, 105  
 Niederste-Ostholt, M., Belokurov, V., Evnas, N.W., Gilmore, G., Wyse, R.F.G., Norris, J.E. 2009, *MNRAS*, 398, 1771  
 Odenkirchen, M. et al. 2003, *AJ*, 126, 2385  
 Ortolani, S., & Rosino, L. 1985, *Mem. Soc. Astron. Italiana*, 56, 105  
 Rosenberg, A., Saviane, I., Piotto, G., Aparicio, A., Zaggia, S.R. 1985, *AJ*, 115, 648  
 Rosenberg, A., Piotto, G., Saviane, I., Aparicio, A., Gratton R. 1985, *AJ*, 115, 658  
 Sarajedini, A., et al. 2007, *AJ*, 133, 1658  
 Schlegel, D. J., Finkbeiner, D. P., & Davis, M. 1998, *ApJ*, 500, 525  
 Spitzer, L., Jr., & Hart, M. H. 1971, *ApJ*, 164, 399  
 van den Bergh, S., Demers, S., & Kunkel, W. E. 1980, *ApJ*, 239, 112

van den Bergh, S. 2000, ApJ, 530, 777

Vesperini, E., & Heggie, D. C. 1997, MNRAS, 289, 898

Whiting, A. B., Hau, G. K. T., & Irwin, M. 2002, ApJS,  
141, 123